Effect of Hard Polymer Filler Particles on Polymer Diffusion in a Low-T_g Latex Film

Jianrong Feng, Ewa Odrobina, and Mitchell A. Winnik*

Department of Chemistry, 80 St. George Street, University of Toronto, Toronto, Canada M5S 3H6

Received January 29, 1998; Revised Manuscript Received June 2, 1998

ABSTRACT: The intercelluar diffusion of poly(butyl methacrylate) (PBMA; glass transition temperature (T_g) = 21 °C) at 60 °C was monitored by fluorescence energy transfer in films formed from blends of PBMA latex and a high-T_g (hard) latex. Two types of hard latexes were used in blends: one composed of poly(methyl methacrylate) (PMMA) and the other having a high-T_g shell made of styrene and acrylic monomer units with a large central void (Rohm & Haas Ropaque, ROP). The diffusion rate of PBMA is significantly decreased in the presence of hard particles. The mean apparent diffusion coefficient (D_{app}) decreased from 0.3 to 0.2 nm^2/s when 35 vol % ROP particles (400 nm) are present in the film and to 0.1 nm^2/s at 75 vol % ROP. The presence of similar-sized PMMA (400 nm) particles showed a slightly larger effect than ROP on the PBMA diffusion: D_{app} decreased by a factor of 2 at 35 vol % PMMA and a factor of 4 at 75 vol % PMMA. At a constant volume fraction of the hard particle additive, the PBMA diffusion rate decreases significantly when the diameter of PMMA particles is reduced from 400 to 67 nm. These effects can be explained in terms of a model in which a more rigid PBMA layer forms, with a slower diffusion rate, near the hard particle surface.

Introduction

Polymer diffusion across interfaces has been an important subject in the areas of welding of polymer slabs,[1] crack healing,[2] sintering of polymer powders by compression molding,[3,4] and the formation and annealing of latex films.[5,6] The diffusion process is directly related to the evolution of mechanical properties.[3,4]

Latex film formation represents a model process for examining polymer diffusion across interfaces. The process involves water evaporation, particle deformation, and fusion of the polymer among particles.[7−9] Voyutskii[7] was the first to emphasize that the forces acting on particle deformation are not sufficient to produce mechanically strong films and that there must be polymer diffusion, in his term as "autohesion", which can lead to healing of the weak boundaries and development of mechanical properties.

Latex films for coatings applications normally contain significant amounts of pigments bound by a latex polymer. These are usually high-modulus (hard) inorganic particles, such as TiO_2, silica, and $CaCO_3$. High-T_g (glass transition temperature) polymeric particles can also serve as an organic pigment in a lower T_g binder resin. One example of this type of polymeric filler is Ropaque (Rohm & Haas), supplied as a dispersion of 400 nm diameter hollow particles with a high-T_g cross-linked styrene−acrylic acid copolymer shell and a central void 250 nm in diameter.[10] When mixed with a latex binder and dried to give a film, the encapsulated air voids provide optimal hiding, an important property for many types of paints, especially architectural coatings.[11] The overall material cost is reduced due to a significant fraction of voids, but the coatings performances can be maintained or even improved. In some cases, for example, in hardwood and automobile coatings, one may wish to obtain transparent films (clear-coats). For this purpose, high-T_g particles, which have a refractive index similar to that of the binder polymer, can be blended into the dispersion. One can obtain transparent films from this type of latex blend, and the mechanical properties are greatly improved due to the presence of hard filler particles.[12]

We are concerned with fluorescent energy-transfer measurements to monitor the polymer diffusion process in latex films. Our intent here is to compare the diffusion rates of a low-T_g polymer in the absence and presence of high-T_g (hard) particles. Poly(butyl methacrylate) (PBMA), having a $M_w = 3.5 \times 10^4$ and a T_g of 21 °C, was used as a model polymer for diffusion. One portion of the PBMA particles was labeled with a fluorescent donor (D) and the other portion with an acceptor (A), both having a mean diameter of 120 nm. In mixtures of these D- and A-labeled particles, we blended different amounts of hard particles, either Ropaque or poly(methyl methacrylate) (PMMA). Diffusion of PBMA in blend films containing hard particles was measured by energy transfer on films annealed at a temperature (60 °C) higher than the T_g of PBMA but much lower than that of the high-T_g particles.

Experimental Section

Latex Samples. Poly(butyl methacrylate) (PBMA) latex samples labeled with 1 mol % of a fluorescent dye [either a donor, phenanthrene (Phe), or an acceptor, anthracene (An)] are referred to as Phe-PBMA and An-PBMA, respectively. These samples were prepared by emulsion polymerization at 80 °C, using potassium persulfate as the initiator and dodecyl mercaptan as the chain-transfer agent, via a semicontinuous process, similar to that described previously.[13,14] The unlabeled poly(methyl methacrylate) (PMMA) particles were also synthesized by emulsion polymerization at 80 °C using potassium persulfate as the initiator.[14] The dispersion of hollow particles (Ropaque OP-62 LO) sample was supplied by Rohm & Haas Co.

The particle size and size distribution were determined by dynamic light scattering employing a Brookhaven BI-90 particle sizer. The size and size distribution for some PMMA samples were also confirmed by scanning electron microscopy (SEM). Molecular weight and molecular weight distribution were measured by gel permeation chromatography (GPC). The glass transition temperatures (T_g) of the polymers were determined by differential scanning calorimetry (DSC) (Perkin-Elmer DSC-7), with a heating rate of 10 °C and under N_2.

S0024-9297(98)00117-X CCC: $15.00
Published on Web 07/25/1998

Table 1. Latex Characteristics

	PBMA[a] 1:1 Phe- + An-labeled	PMMA				ROP
diameter (nm)	120	67	107	140	400	≈400
T_g (°C)	21		105			high
M_w (×10⁴)	3.5	50	37			
M_n (×10⁴)	1.7	20	16			

[a] The particle size, T_g, and molecular weight for Phe-PBMA are very similar to those for An-PBMA, and the values here are from a 1:1 mixture of Phe- and An-labeled particles.

Some important characteristics for the various latex samples used are listed in Table 1. The PBMA latex has a diameter of 120 nm, a T_g of 21 °C, and a random dye distribution in the polymer molecules.[14] Four PMMA samples ($T_g \sim 105$ °C), with different particle sizes ranging from 67 to 400 nm in diameter, were used. The Ropaque (ROP) latex, made of styrene with a significant fraction of acrylic acid monomers, has a $T_g > 100$ °C in the dry state, but its T_g may be lower under wet conditions. We were unable by DSC measurements to observe a T_g transition between −20 and +150 °C for a dried ROP sample. The particles have an average diameter of ca. 400 nm and a central void 250 nm in diameter. Thus, the polymer in the shell represents 74% of the total particle volume. All the latex samples had a narrow particle size distribution, as indicated by dynamic light scattering (DLS) and electron microscopy measurements.

Film Formation and Measurements. All the dispersions, including PBMA, PMMA, and ROP, were cleaned by an ion-exchange resin (AG-501-X8 mixed-bed resin, Bio-Rad) to remove the ionic surfactant and other ionic species before film formation. After ion exchange, the pH of all the latex samples decreased from 8−9 to 5−6, including the ROP sample, indicating the protonation of the surface acids (−SO_4H for PBMA and PMMA and −COOH for ROP) and the removal of some ionic and basic species. Latex films were prepared from dispersion mixtures of 1:1 number ratio (N_{Phe}/N_{An}) of Phe- and An-labeled PBMA particles and varying volume fractions (Φ_{hard}) of hard particles (PMMA or ROP). The volume ratios in blends were calculated based on the weights of solids of the various types of particles, using density values of 1.05 g/mL for PBMA, 1.15 g/mL for PMMA, and 0.75 g/mL for dry ROP. Film formation was carried out at 28 °C on quartz plates covered by an inverted Petri dish in an oven with air circulation, with a drying time of about 3 h. The films had a typical thickness of 100 μm. After drying, crack-free films were obtained for blends with a volume fraction of hard particles Φ_{hard} lower than about 0.55. The films with high Φ_{hard} (e.g., 0.75) had small cracks, but they could be placed vertically in the sample chamber of our instrument for spectroscopic measurements. The ROP-filled films were opaque white at all compositions ($\Phi_{hard} > 0$), due to the air voids in the hard particles. Films containing PMMA microspheres gave transparent films at low pigment concentration ($\Phi_{hard} = 0.1-0.35$) for various PMMA particle diameters (67−400 nm). This indicates that the PBMA sample serves as a good binder to form void-free blend films and that the PMMA particles are well dispersed in these films.[12] Unlike ROP, PMMA has a refractive index similar to that of PBMA (1.49 vs 1.48).[12] The dried films were stored in sealed test tubes at −10 °C in the freezer to arrest diffusion until annealing experiments were carried out. Films were then annealed at 58 ± 1 °C for polymer diffusion measurements. For each series of samples for comparison, the films were dried and annealed simultaneously. Figure 1 shows schematically the formation and annealing processes for a film prepared from a blend of PBMA (1:1 Phe- + An-labeled) and ROP particles.

Fluorescence decay profiles were measured by the single-photon-timing technique.[15] The measurement conditions were similar to those described in ref 5. After each time interval of annealing, the fluorescence decay profile of each film is measured. Each measurement took about 4−5 min to collect 3500 counts in the maximum channel, corresponding in the experiment to 2−3 decades of fluorescence decay.

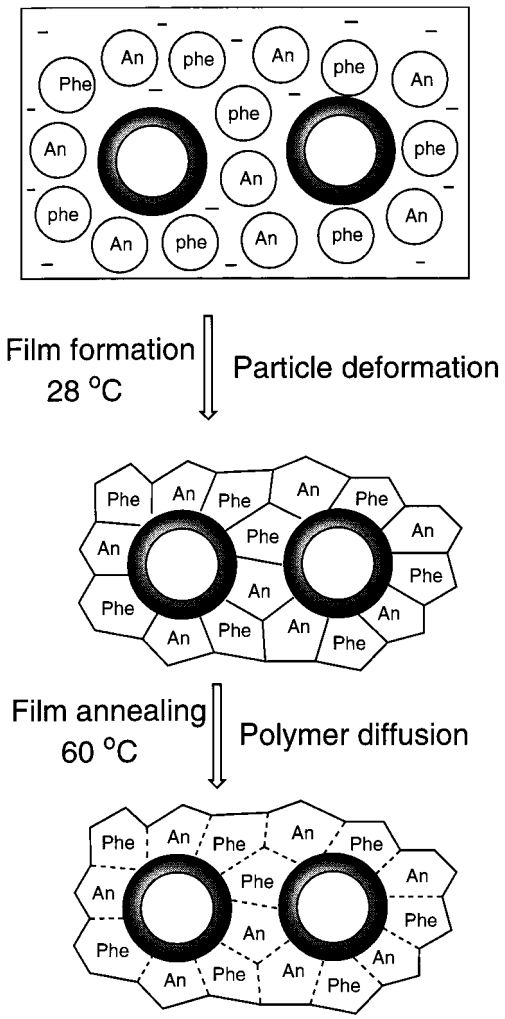

Figure 1. Schematic representation of the formation and annealing processes for a film prepared from a blend of PBMA (1:1 Phe- + An-labeled) and larger hollow (ROP) particles. The shell (dark region) of ROP has a high T_g, and the ROP particles serve as a hard filler in the PBMA matrix. A similar situation pertains to blends of PBMA and PMMA microspheres, except that the PMMA particles are solid.

Results and Discussion

Energy Transfer and Diffusion Analysis. When donor (D) and acceptor (A) chromophores are sufficiently close, the excited donor can transfer its energy to the acceptor in competition with its spontaneous radiative and radiationless decay processes. The efficiency of energy transfer (Φ_{ET}) can be determined from the area under the donor fluorescence decay profile $I_D(t')$ from samples containing both D and A.[5] For a film sample allowed to anneal, the area under the decay curve and Φ_{ET} evolves with annealing time t.

$$\Phi_{ET}(t) = 1 - \text{area}(t)/\tau_D^\circ \quad (1)$$

where $\tau_D^\circ \sim 45$ ns is the unquenched lifetime of the phenanthrene decay in many acrylic polymer films. To obtain an accurate area(t) under each decay profile, the mathematical decay function in eq 2 was used to fit the decay curve, and the area was obtained by integrating $I_D(t')$ from decay time $t' =$ zero to $t' =$ infinity.

$$I_D(t') = A_1 \exp[-t'/\tau_D^\circ - p(t'/\tau_D^\circ)^{1/2}] + A_2 \exp(-t'/\tau_D^\circ) \quad (2)$$

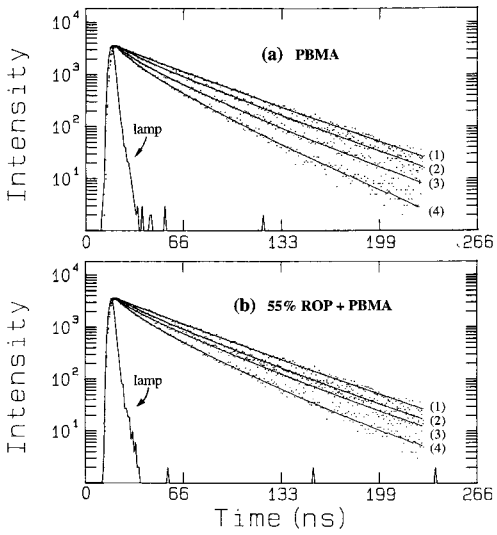

Figure 2. Donor fluorescence decay profiles for latex films annealed at 58 ± 1 °C for 0 min (curves 1), 10 min (curves 2), 40 min (curves 3), and 190 min (curves 4). In part a we show the data for a pure PBMA (1:1 Phe- + An-labeled) film. The profiles in part b are for a blend of PBMA with 55 vol % ROP. Both samples were annealed simultaneously. In our data analysis, these curves are integrated to obtain their areas.

The fitting parameters A_1, A_2, and p in eq 2, obtained from fitting to each decay profile, are useful for area integration, but their physical meaning is not important here.

Both the area under the decay curve and Φ_{ET} are useful parameters to characterize the diffusion process upon annealing. Another parameter is the extent of mixing, $f_m(t)$, expressed in terms of the growth in energy-transfer efficiency normalized by the maximum change associated with complete mixing[5]

$$f_m(t) = \frac{\Phi_{ET}(t) - \Phi_{ET}(0)}{\Phi_{ET}(\infty) - \Phi_{ET}(0)} = \frac{\text{area}(0) - \text{area}(t)}{\text{area}(0) - \text{area}(\infty)} \quad (3)$$

where $[\Phi_{ET}(t) - \Phi_{ET}(0)]$ represents the change in ET efficiency between the initially prepared film and that annealed for time t. The term $f_m(t)$ is useful for characterizing the extent of polymer diffusion measured by the ET technique.

Fluorescence decay measurements were carried out on our film samples as a means of assessing the extent of energy transfer as a function of annealing history and of film composition. Figure 2 shows examples of two series of donor decay data. In Figure 2a we present the profiles for a PBMA film without high-T_g filler particles annealed at 58 °C for 0, 10, 40, and 190 min, respectively. The profiles in Figure 2b are for a PBMA film filled with 55 vol % ROP particles after annealing for the same time intervals at 58 °C as in Figure 2a. As seen in Figure 2, when the films are annealed, the curvature of the decay profiles becomes more pronounced and the area under the decay curves decreases. Molecular mixing between donor- and acceptor-labeled polymers increases the extent of energy transfer, leading to faster decay of the donor fluorescence.

The extent of mixing expressed in terms of the fractional growth of ET efficiency, $f_m(t)$, can be obtained via eq 3 by comparing the areas under the decay profiles for films annealed for various times [area(t)] to that of a film without annealing [area(0)] and to one annealed for a sufficiently long time to approach the minimum value of the area [full mixing, area(∞)].

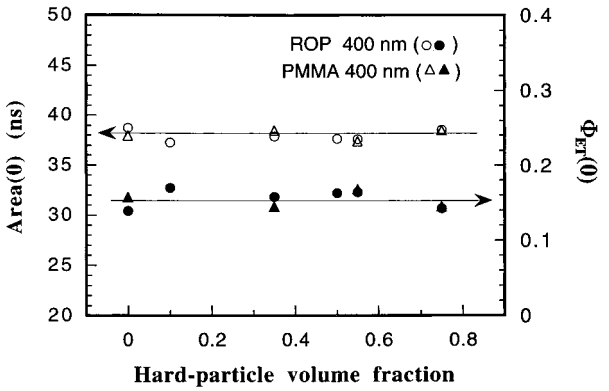

Figure 3. Plots of area(0) (unfilled symbols) and $\Phi_{ET}(0)$ (filled symbols) vs the hard-particle volume fraction (Φ_{hard}) for various nascent films [pure PBMA, blends of PBMA with ROP (circles), and blends of PBMA with PMMA (triangles)].

Initial Energy Transfer in Nascent Films. To interpret Φ_{ET} values, one needs first to distinguish the amount of energy transfer that occurs between D and A groups on opposite sides of particle−particle interfaces in newly formed films from the much larger extent of ET that occurs as the polymer molecules diffuse across the interface and mix. The interfacial contribution to ET is measured by area(0) determined from the donor decay profile of a film after drying a sample at a temperature (here 28 °C) above its minimum film-forming temperature and storing the film below its T_g before the measurement. Examples of the decay profiles for such films are shown in Figure 2 as curve 1 in both series of data.

We have found that the amount of energy transfer in the nascent films is related to the relative ratio of the D−A interfacial area to the volume of the D-labeled phase.[14,16] Here we are interested in the $\Phi_{ET}(0)$ values, which provide a measure of the interfacial area of the system, for films formed from different PBMA/hard-particle blend compositions. In Figure 3 we plot the area(0) and $\Phi_{ET}(0)$ vs the hard-particle volume fraction (Φ_{hard}) for various film samples (pure PBMA, PBMA + ROP, and PBMA + PMMA). One notices that the amount of ET is almost independent of the hard-particle fraction from $\Phi_{hard} = 0$ to $\Phi_{hard} = 0.75$, with the area(0) ranging from 37.4 to 38.7 ns, corresponding to $\Phi_{ET}(0)$ varying from 0.17 to 0.14. The range of variation of area(0) is rather small, but the scatter in $\Phi_{ET}(0)$ values introduces uncertainties in evaluating the interfacial areas. Nevertheless, there is no trend for changes in $\Phi_{ET}(0)$ over a wide composition range; rather, a flat line can be drawn through all the data points in Figure 3. These $\Phi_{ET}(0)$ values are quite close to those we obtained for similar PBMA films examined independently. This indicates that the ratio of the D/A interfacial area to the volume of the D-labeled particles does not change significantly, even when a large fraction of unlabeled hard particles is present. In filled films, a significant fraction of the surface area of most of the D-labeled particles must be in contact with filler particles (cf. Figure 1), where no ET takes place. The above result implies that the mean surface area of each PBMA particle is increased as more hard particles are incorporated into the film, so that the presence of PBMA/hard-particle contacts does not decrease significantly the

interfacial area between D- and A-labeled PBMA particles.[17−19]

Because the PBMA soft latex component we examine here has a low molecular weight and a T_g (21 °C) close to room temperature, polymer diffusion takes place slowly at room temperature. If the extent of this diffusion were significant, it would affect the magnitude of the area(0) [or $\Phi_{ET}(0)$] we determine. In previous experiments with this latex sample,[14] we have shown that there is a clear onset of interparticle polymer diffusion that occurs only after the sample is dry, i.e., after the sample has reached >90 wt % solids. On a flat substrate, these dispersions dry as a moving front, to yield a film with a transparent dry outer perimeter surrounding a turbid wet zone that decreases in size as the drying proceeds. If the film samples are not too large, the extent of diffusion that has occurred when the last vestiges of the wet zone disappear can be neglected in our analysis. However, these films must be removed from the 28 °C oven and rapidly quenched to −10 °C to prevent this diffusion. These experiments require a sharp eye and a deft hand because films formed from dispersions with different amounts of hard particles dry at different rates.[12] The data in Figure 3, for example, were obtained from two sets of experiments, in which all films were dried under the same conditions (in the same covered dish) but each film was removed from the oven immediately after completion of drying at 28 °C. We observed that the films with $\Phi_{hard} = 0.35-0.55$ dried slower than those with $\Phi_{hard} = 0-0.1$ and $\Phi_{hard} = 0.75$, with drying times of about 3 h vs 3.5−4 h. This difference in drying rate (slowest at intermediate Φ_{hard}) is consistent with the mechanism of drying in latex blend dispersions described previously.[12] Other experiments showed that if all the films were removed from the oven after the slowest sample had dried, Φ_{ET} values for the samples that dried fastest had increased to 0.19−0.20.

Maximum Energy Transfer in Well-Mixed Films. The above results indicate that, for a given volume of PBMA, the total interfacial area available for interdiffusion between D- and A-labeled molecules is similar, even when a high fraction of filler particles is incorporated into the blend. To examine whether the filler particles were able to suppress diffusion for some fraction of the polymer, we examined the effect of long annealing times on the extent of polymer diffusion. We measured the extent of energy transfer for films of different blend compositions annealed for sufficiently long times ($t \rightarrow \infty$) that the Φ_{ET} values approached their maximum value $\Phi_{ET}(\infty)$. At this point, the diffusion approaches its final, equilibrium state where all the D- and A-labeled molecules are well-mixed.[24] Because of the relatively low molecular weight of our PBMA sample, we could anneal the films at relatively low temperatures (60 °C) for relatively short times, ranging from a few hours to 1−2 days, and still allow the samples to reach $\Phi_{ET} \approx \Phi_{ET}(\infty)$. Figure 4 shows plots of area(∞) and $\Phi_{ET}(\infty)$ vs the hard-particle volume fraction (Φ_{hard}) for various well-annealed PBMA latex films (pure PBMA, PBMA + ROP, and PBMA + PMMA). One sees that the area(∞) values for the blends are slightly higher than that for pure PBMA, and the $\Phi_{ET}(\infty)$ values also show a slight decrease with increasing Φ_{hard}. These differences are rather small, with the area values ranging from 13.6 to 15.2 ns and the Φ_{ET} values from 0.70 to 0.66. Note that these differences

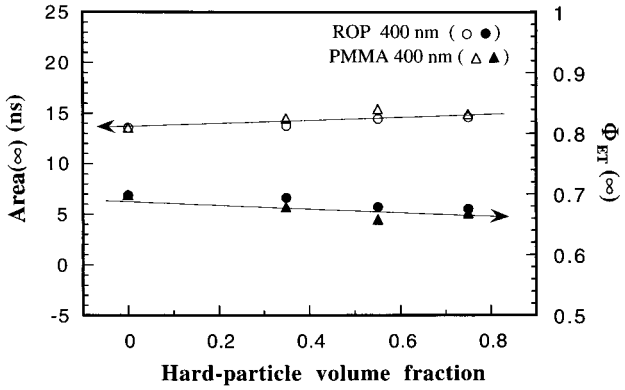

Figure 4. Plots of area(∞) (unfilled symbols) and $\Phi_{ET}(\infty)$ (filled symbols) vs the hard-particle volume fraction (Φ_{hard}) for various PBMA films blended with ROP (circles) and with PMMA (triangles).

would be even smaller if we extended the measurements to longer annealing times. We find that the time needed for a film to reach high Φ_{ET} is much longer for films with higher Φ_{hard} than for those with lower Φ_{hard}. For example, to reach $\Phi_{ET} \geq 0.66$, ca. 3 h for pure PBMA and 22−30 h for the $\Phi_{hard} = 0.75$ samples are required. It is difficult in a film with high Φ_{hard} for the energy-transfer efficiency to reach its limiting $\Phi_{ET}(\infty)$ value. Nevertheless, it is clear that all the above samples undergo sufficient interdiffusion to reach close to their full-mixing state, with the ET efficiencies similar to, or even somewhat higher than, what we normally obtain with higher molecular weight PBMA films with the same dye concentrations (area 13.6−15.2 ns vs 15−20 ns). The small differences in the area and Φ_{ET} values among the well-annealed films are not considered to be significant in our data analysis, and they do not interfere with our comparison of diffusion rates for the different samples examined here.

Our main objective in this study is to compare the rates of intercelluar polymer diffusion for PBMA in latex films containing different amounts of hard-particle additive. The fact that we find similar area(0) and area(∞) values for the samples we wish to investigate is particularly helpful for comparison of their diffusion rates. Interparticle polymer diffusion for all of these samples starts at a similar value of $\Phi_{ET}(0)$ and evolves to a similar state of mixing [$\Phi_{ET}(\infty)$] as perceived by the energy-transfer experiment. These similarities facilitate comparison of the relative polymer diffusion rates through examination of the rate at which Φ_{ET} and f_m increase with annealing time from their initial to their asymptotic values.

In normal practice, area(∞) can also be obtained from a film of the same composition but cast from an organic solution. For the PBMA sample here, area(∞) was obtained by comparison of the value obtained for a film annealed at 60 °C for 4 h with that of a film of identical composition prepared by solvent-casting. These two types of samples gave similar decay profiles, but the integrated area value from the annealed sample (13.6 ns) was slightly lower than that from solvent-casting (15.0 ns). Thus, 13.6 ns was chosen as the area(∞) for our film samples. The initial area(0) was simply taken as the average from various samples in Figure 3, with a value of 38.2 ns. We use the f_m parameter, calculated based on the areas under the decay curves, as a measure of the extent of diffusion in our annealed latex films. Representative data of f_m values for our films as a

function of annealing time will be presented in the following sections.

To proceed more deeply into the analysis of the diffusion process, one needs to calculate the diffusion coefficient of the polymer, characterizing the rate of movement of the polymers across the interparticle interface. This can be done at different levels of rigor and sophistication.[20−22] In our case, the diffusion coefficients were calculated by fitting the f_m data obtained from energy transfer to a spherical diffusion model which satisfies Fick's laws of diffusion.[23] The details of this analysis, its convenience, and its shortcomings have been described previously.[5d] The diffusion coefficients we obtained are apparent mean diffusion coefficients D_{app}, averaged over all the chains in the sample and the annealing history of the film.

Effects of Hard Particles on PBMA Diffusion. In this section we examine the diffusion rates of PBMA at 60 °C in films containing different amounts of hard particles and containing hard particles of different size. Our analysis implicitly assumes that since both PMMA and the cross-linked ROP particles are glassy at 60 °C, no significant PBMA diffusion into the filler particles occurs. Some experiments with labeled hard particles have been carried out and appear to confirm this hypothesis.[16] Further confirmation is provided by the similar $\Phi_{ET}(\infty)$ values found for all blend film samples, even those with $\Phi_{hard} = 0.75$, annealed for long times at temperatures below the T_g of the hard component. This result indicates that the volume of the PBMA phase and the final average dye concentrations do not change when hard particles are present.

Effect of ROP Particles. Examples of donor decay profiles for PBMA films with and without ROP are shown in Figure 2. With a sharp eye, one can see that curve (4) in Figure 2a decays more rapidly than the corresponding curve in Figure 2b. This result indicates that, for the same thermal history, less intercellular polymer mixing has occurred for PBMA in the presence of ROP. We analyze these decay curves as described above and plot the results in Figure 5 of PBMA films blended with different amounts of ROP. In Figure 5a we plot the extent of mixing (f_m) vs annealing time, and in Figure 5b we plot the calculated apparent diffusion coefficient (D_{app}) vs f_m. One sees that, in films containing increasing amounts of ROP particles, the rate of increase of the extent of mixing becomes slower. The D_{app} values are on the order of 0.3 nm^2/s in the pure PBMA sample, 0.2 nm^2/s in the 35 vol % ROP sample, and 0.1 nm^2/s in the 75 vol % ROP sample. These results indicate that the presence of ROP filler can decrease significantly the diffusion rate of the surrounding polymer.

Effect of PMMA Particles. Figure 6 shows the PBMA diffusion data for films blended with different amounts of 400 nm diameter PMMA particles. In Figure 6a we plot the extent of mixing (f_m) vs annealing time, and in Figure 6b we plot the apparent diffusion coefficient (D_{app}) vs f_m. One sees that with an increase in the amount of PMMA particles the growth rate of f_m becomes slower, similar to the effect from ROP. The D_{app} values decrease from ca. 0.3 nm^2/s in pure PBMA to 0.2−0.15 nm^2/s in the 35 vol % PMMA sample, to 0.12−0.1 nm^2/s in the 55 vol % PMMA sample, and to 0.08−0.06 nm^2/s in the 75% PMMA sample. A decrease in D_{app} values as large as a factor of 4 is observed. These results indicate that the presence of PMMA particles decreases significantly the diffusion rate of polymer molecules in the surrounding matrix. When

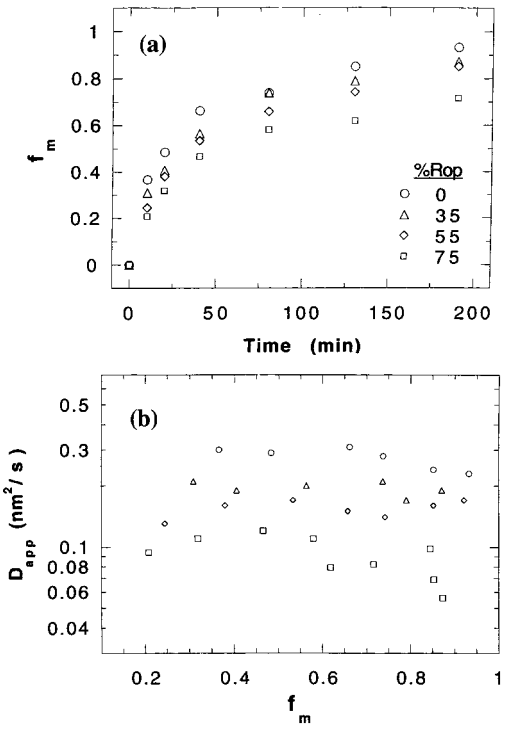

Figure 5. Comparison of PBMA diffusion rates for films blended with different amounts of ROP particles, expressed as volume percent (% ROP): 0 (circles), 35 (triangles), 55 (diamonds), and 75 (squares), respectively. In part a we plot the extent of mixing (f_m) vs the annealing time, and in part b we plot the apparent polymer diffusion coefficient (D_{app}) vs f_m.

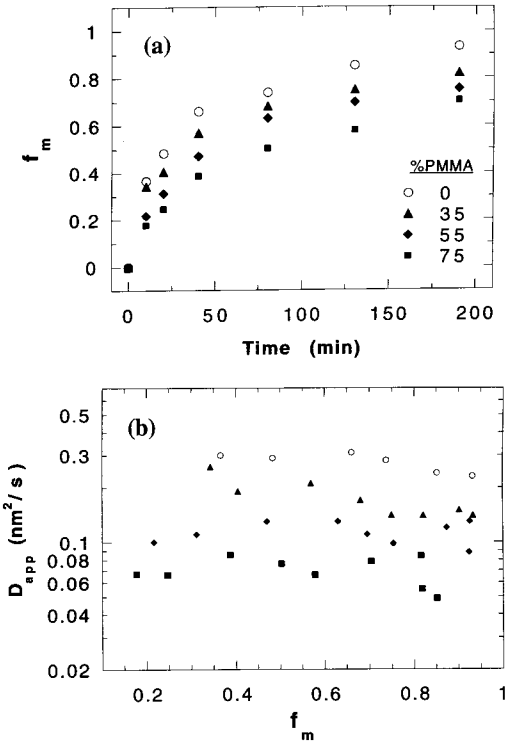

Figure 6. Comparison of PBMA diffusion rates for films blended with different amounts of 400 nm diameter PMMA particles (% PMMA): 0 (circles), 35 (triangles), 55 (diamonds), and 75 (squares), respectively. In part a we plot f_m vs time, and in part b we plot D_{app} vs f_m. We use filled symbols for these PMMA-containing samples to distinguish them from ROP-containing samples.

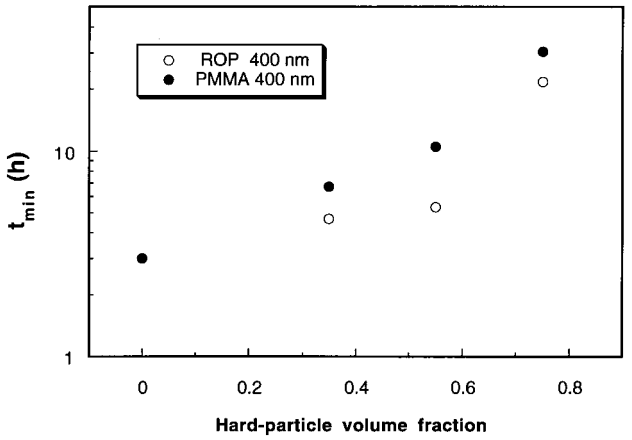

Figure 7. Plot of the minimum time (t_{min}) taken to reach $f_m > 0.95$ ($\Phi_{ET} > 0.66$) vs the blend composition (Φ_{hard}), for PBMA/ROP (unfilled symbols) and PBMA/PMMA (filled symbols) films.

we compare results for the ROP- and PMMA-filled films, with both experiments carried out simultaneously, we find similar effects, except that PMMA consistently gives greater retardation of the diffusion of PBMA than ROP particles of similar size.

In Figures 5a and 6a we present data only for f_m values up to an annealing time of 190 min for all films, for easy visualization of the differences among the samples of various compositions. In fact, we continued these measurements until f_m in all samples approached unity, corresponding to the $\Phi_{ET}(\infty)$ data (0.66−0.70) shown in Figure 4. At high extents of mixing, our calculation of D_{app} is subject to large errors.[21] One way of comparing relative diffusion rates at long times for samples with different compositions is the minimum time (t_{min}) taken for each sample to reach $f_m \approx 1$ ($\Phi_{ET} \geq 0.66$). In Figure 7 we plot t_{min} vs the blend composition (Φ_{hard}). One sees that at large Φ_{hard} it requires a much longer time for the film to diffuse to a well-mixed state than at low Φ_{hard}. To reach $\Phi_{ET} = 0.66$ (area = 15.5 ns), ca. 3 h for pure PBMA, 5−7 h for the $\Phi_{hard} = 0.35$ samples, 6−10 h for the $\Phi_{hard} = 0.55$ samples, and 22−30 h for the $\Phi_{hard} = 0.75$ samples are required. It took even longer, up to 45 h, for a $\Phi_{hard} = 0.75$ sample to increase its Φ_{ET} further to 0.68 (area = 14.5 ns). These results clearly show that the mixing process is much retarded by the hard particles. When the data are plotted in this way, the larger influence of PMMA on retarding the diffusion of the matrix polymer can be seen more clearly.

Variation of the Hard-Particle Size. Effects of a filler on the mobility of the surrounding matrix are likely due to an interaction of the matrix with the surface of the filler particles. To test this idea, we examined PBMA diffusion rates in films blended with PMMA at a fixed volume fraction but different hard-particle diameters (d_{PMMA}). Figure 8 shows the PBMA diffusion data for a pure PBMA film and for films blended with 35 vol % PMMA particles of different diameters, i.e., d_{PMMA} = 400, 140, 109, and 67 nm, respectively. A very interesting result is observed in this figure: the diffusion rate is increasingly retarded with decreases in the size of the hard particles. Here pure PBMA has D_{app} values on the order of 0.3 nm^2/s, close to those shown in Figures 5 and 6 measured in another set of experiments, reflecting the consistency of the experiments.[24b] The D_{app} values decreased to 0.2 nm^2/s in the d_{PMMA} = 400 nm sample and 0.06 nm^2/s in the d_{PMMA} = 67 nm sample. A difference factor of 5 in the D_{app} values is found between a pure PBMA and that blended with 67 nm PMMA particles.

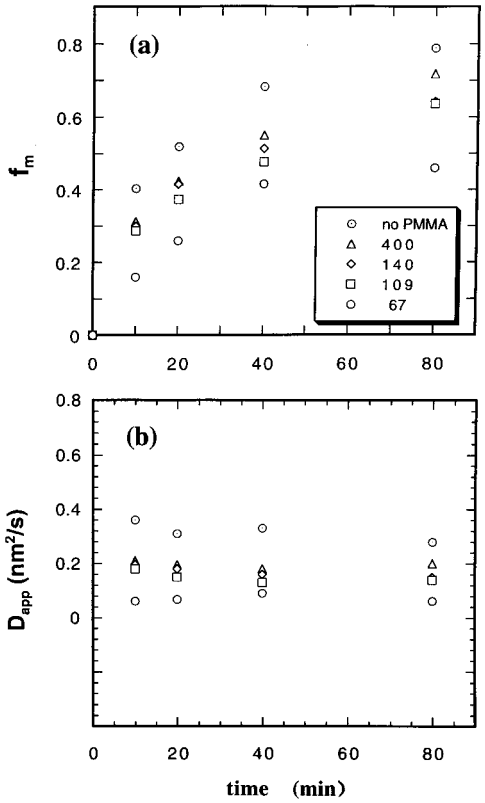

Figure 8. Comparison of PBMA diffusion rates for a pure PBMA film (⊙) and for films blended with 35 vol % PMMA particles of different diameters (d_{PMMA}): 400 nm (△), 140 nm (◇), 109 nm (□), and 67 nm (○). In part a we plot f_m, and in part b we plot D_{app} vs the annealing time.

Models for Effects of Hard Filler on Polymer Dynamics. The above results indicate that the presence of hard filler particles significantly decreases the diffusion rate of a low-T_g polymer. One can envision many possible explanations for this effect. First, those polymers with polar groups (e.g., PBMA) can have significant interactions (e.g., hydrogen bonding) with filler particles near the hard-particle surface, particularly with those hydrophilic or ionic particles (e.g., silica, TiO_2, etc.), which might influence the polymer diffusion rate. Solid substrates decrease the diffusion coefficient of polymers in thin-film (5 nm) polymer melts, and the magnitude of the effect depends on the nature of the substrate−polymer surface.[25] In our case, the ROP particles contain a significant amount of −COOH groups and should have good H-bond donor capacity, while the PMMA particles have a very low level of surface acid ($-SO_4H$) groups (on the order of 0.1 $-SO_4H$/nm^2). We found the PBMA diffusion rate for a PMMA-filled sample is similar to, but further retarded than, that for ROP-filled samples with the same composition and similar hard-particle size. Since we do not have detailed knowledge about the ROP particle surface, we cannot at this point comment on what types of interactions take place at the soft polymer−hard filler interfaces.

Current Views on Polymer−Filler Interaction. It is well-known that adding a hard filler to a polymer matrix has a profound effect on the mechanical properties of the composite blend. The most common type of

polymer−filler system is a polymer resin reinforced by addition of a high modulus filler, such as glass beads, carbon-black, or high-modulus polymeric particles. It is often found that not only do the two components (filler + polymer) display their own properties (e.g., modulus) in the composite but also, through their interactions, many properties of the matrix polymer are modified. Many experiments indicate that the presence of the filler leads to a layer of soft polymer matrix near the hard surface that has reduced mobility or higher rigidity compared to its properties in bulk. We still know relatively little about the width of this rigidified layer, how its properties evolve with distance from the interface, and how they depend on specific interactions occurring at that interface.

NMR relaxation time measurements describing changes in the matrix phase of filled rubbery polymers have been reported over the last 2 decades.[26−28] These experiments revealed the existence of polymer regions characterized by low mobility. In the immediate vicinity of the particle surface, there was a polymer layer with a very low spin−spin relaxation time (T_2), which did not change significantly when the sample was heated through the rubber glass transition. This layer was essentially immobile on the time scale of the measurement. The material beyond this layer had a T_2 value measured at temperatures above the T_g that was 1 order of magnitude lower than the T_2 of the unfilled rubber. This difference was attributed to the existence of a layer of restricted mobility. Douglass et al.[26b] calculated the thicknesses of the two layers using an equation derived by Pliskin and Tokita.[29] Generally, the thickness of the immobile layer varied between 0.5 and 2 nm with an average of ca. 1.5 nm, while the restricted mobility layer was between 2.5 and 9 nm thick (on average 6.6 nm), depending on the size and volume fraction of carbon-black particles.[26,29] One should note that the immobile, bound layer was originally believed to arise from both chemical bonding and "permanent" physical attachment, and its thickness was estimated by the amount of polymer remaining after exposure to an organic solvent.[26,29]

A number of important experiments on filled polymer systems by several investigators[30−32] have employed dynamic mechanical analysis (DMA). In various polymer systems filled with a significant fraction of rigid particles (carbon-black, silica), two glass transitions were inferred, as indicated by two peaks in the tan δ vs temperature plot. The first peak (T_{g1}) occurred at the normal T_g of the pure polymer. The second broad peak (T_{g2}) appeared at 40−100 °C higher temperature and was assigned to the glass transition of regions of restricted mobility. Tsagaropoulos and Eisenberg[32] examined various polymers filled with fine silica particles and found that the existence of a second T_g transition related to reduced mobility was indeed a general phenomenon. They also observed that the area under the higher-T_g peak in the tan δ plot decreased with an increase in the filler concentration and suggested that this change was due to creation of an increasing fraction of an immobilized polymer layer whose response was not detectable by DMA. According to Tsagaropoulos and Eisenberg,[32] the immobilized region could be a major fraction of the total polymer volume at a filler content > 20 wt %, much larger in size than that found by McBrierty et al.[26] and Pliskin et al.[29] On the basis of the work by McBrierty et al., Tsagaropoulos and Eisenberg[32] proposed a two-layer model in terms of mobility: a tightly bound, immobilized layer at the hard filler surface and a loosely bound layer with restricted mobility around the immobilized layer. At high filler content, the loosely bound layers of reduced mobility overlap and then become even less mobile. If the filler content is not very high, a significant fraction of polymer remains outside these layers. It maintains its bulk polymer properties and exhibits a normal T_g.

Another set of experiments examined Young's modulus in systems with filler particles of different sizes.[33−36] It was shown that Young's modulus (E) tended to increase with a decrease in filler particle size, consistent with the idea that the interaction between the polymer and filler are related to the surface area of the hard filler material. Vollenberg et al.[36] proposed a two-layer model to explain the results. In their picture there was also a rigid (high-modulus) polymer layer adjacent to the filler surface, which was interpreted as arising from the formation of a high density of material in this region ($E \propto \rho^7$ according to van Krevelen[37]). They also thought that around the high-E layer there was a thin, less-dense layer which had a lower modulus than the bulk.

In polymer films with thicknesses on the order of a few hundred angstroms, one finds that the film surface effects the measured T_g. On the basis of ellipsometry measurements, Keddie et al.[40] reported that a thin PMMA film has a slightly higher T_g on an SiO_2/Si substrate than in bulk. On Au surfaces, with which polar interactions are minimal, the T_g is lower. Neutron and X-ray reflectivity studies of thin supported polymer films also show an increase in T_g values with a decrease in film thickness.[41] A key insight into the underlying physics was provided by Dutcher and co-workers,[42] who measured T_g for thin free-standing polystyrene films by Brillouin scattering and showed that the free air surface was responsible for the lowering of T_g. They cite molecular dynamics simulations[43,44] that suggest that the effect of the free surface is to enhance the mobility of the polymer chains near the polymer−vacuum interface, whereas the presence of confining but noninteracting walls results in an increase in density and a decrease in polymer mobility over distances that extend beyond the radius of gyration of the polymers. The authors[42] argue that for substrate-supported polymer films one may observe either a higher T_g or a lower T_g depending upon whether the effect of the substrate or the free surface dominates. A summary of this work recently appeared.[45]

Surface effects on polymer diffusion were alluded to above in ref 25, where the authors examined the rate of diffusion of 50 Å films of polystyrene (PS) into a matrix of deuterated PS and found that proximity to the SiO_2/Si surface retarded the diffusion rate in a manner consistent with increased friction from monomer substrate contacts. When the substrate was first passivated with poly(vinylpyridine), the effect was much smaller. In these experiments, the polymer diffused away from the substrate into a matrix of much greater thickness. The effect of film thickness on diffusion in the plane of the substrate was reported by Frank et al.,[46] who used fluorescence recovery after pattern photobleaching (FRAPP) to study the tracer diffusion of polystyrene labeled with a fluorescent dye. They found a substantial decrease in the diffusion rate for films thinner than 1500 Å.

Chart 1

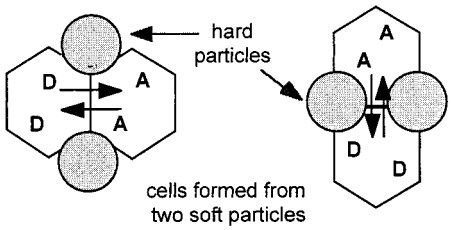

It is on the basis of these results that we believe that the retardation in polymer diffusion rates that we observe is due to surface interactions between the hard latex particles and the lower T_g polymer, whose mixing we study by energy transfer.

An astute reviewer has asked us to consider the possibility that the retardation in mixing rates determined from energy-transfer experiments is due to the added hard particles acting as obstacles. This reviewer points out that at 35 vol % solids the *average* interparticle distance is 135 nm for the 109 nm diameter hard particles and 83 nm for the 67 nm diameter particles. Obstacles decrease the apparent diffusion rate by increasing the tortuosity of the diffusion path. Free-volume models ascribe the decreased diffusion rate to an increase in the microscopic friction coefficient, whereas tortuosity increases the diffusion path length without affecting the friction coefficient. Obstacle effects can be very important in latex films and other paint films. For example, obstacle effects retard the evaporation of water from latex films containing a mixture of hard and soft particles.[12b] In addition, the solvent evaporation rate from solvent-cast films containing inorganic pigment can be explained in terms of the pigment acting as obstacles to increase the path length traveled by the solvent molecules as they diffuse through the film to the air−film surface.[47]

An image representing this reviewer's point of view is shown on the right-hand side of Chart 1 for the case where the hard particle has a diameter smaller than that (120 nm) of the soft latex particles which form the film. This reviewer believes that in our experiments the hard particles operate to constrain the rate of mixing of donor- and acceptor-labeled latexes, much as a narrow pipe limits the flow of liquid.

Our view is different. We are influenced by the data in Figure 3 and other results which indicate that the presence of the hard particles does not significantly affect the interfacial area between the donor- and acceptor-labeled cells in newly formed films. These are the interfaces across which the diffusion we measure occurs. One characteristic feature of obstacle effects on diffusion is that the characteristic diffusion length is larger than the size of the obstacles. The mixing we observe in our energy-transfer experiment operates over a very short length scale. By the time the polymer molecules have diffused a distance corresponding to one particle radius, the mixing detected by energy transfer is virtually complete. We depict this process on the left-hand side of Chart 1.

In latex films formed from a blend of hard and soft particles, the hard particles are not necessarily distributed randomly in the matrix. We know from the work of Eckersley and Helmer[48] that small hard particles in a film formed from a blend with larger soft particles are not distributed uniformly. Rather, they tend to form chains which can form a percolation network which serves to reinforce the film. The hard particles not only increase the modulus of the film at low strain but also increase the tensile strength of the film.

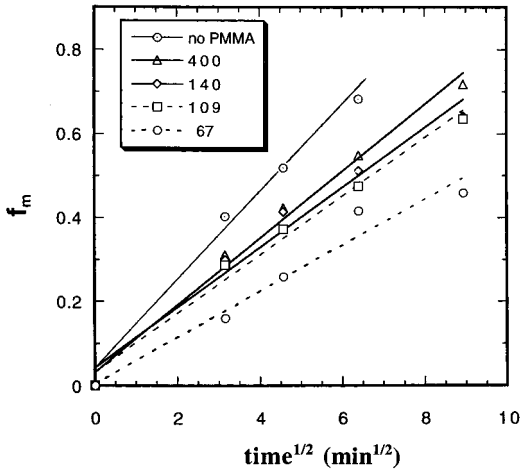

Figure 9. Plots of f_m vs $t^{1/2}$ for a pure PBMA film (⊙) and for films blended with 35 vol % PMMA particles of different diameters (d_{PMMA}): 400 nm (△), 140 nm (◇), 109 nm (□), and 67 nm (○), respectively. The data were derived from Figure 8a using f_m values ≤ 0.7.

While we accept the possibility that future experiments may reveal the importance of obstacle effects, we prefer at this time to interpret our data in terms of a model in which the surface of the filler particles serves to make the adjacent matrix more rigid.

Model for Analysis of Diffusion Data. Our results on PBMA diffusion indicate that the diffusion rate depends on the surface area of the hard particles, as shown in the f_m vs t plots or the D_{app} vs f_m plots in Figure 8. Another way to compare these diffusion rates is to plot f_m as a function of $t^{1/2}$. For diffusion which follows Fick's laws one expects mixing to increase with $t^{1/2}$. For this low molecular weight PBMA sample and for many other samples we have studied, we find that a linear plot of f_m vs $t^{1/2}$ can be obtained for f_m values approaching 0.7.[5,14] Figure 9 shows the f_m vs $t^{1/2}$ plots for a PBMA film and for PBMA/PMMA blends with various PMMA particle diameters (d_{PMMA}). All of the samples give reasonable linear plots. The data can be fitted to straight lines which are forced to pass through the origin, but in the analysis that follows, we compare the slopes of the least-squares best fits to the lines as shown in Figure 9. We ignore the small positive intercepts at $t = 0$ with $f_m \leq 0.04$.

To proceed with our data analysis, we define a diffusion rate parameter k, characterizing the rate of diffusion, as the slope in the f_m vs $t^{1/2}$ plot. In pure PBMA, the increase in f_m can be described by a single rate parameter $k°$.

$$f_m = k°t^{1/2} \tag{4}$$

In blends of PBMA with hard particles, the situation is more complex. There are regions of PBMA with different mobilities. These are characterized by different diffusion rates (different k values). On the basis of the models presented in the literature by McBrierty, Eisenberg, Vollenberg, and others, we propose a simple model to rationalize the effects of hard particles on the diffusion rates we measured (Figure 10). We assume that in blends there is a PBMA layer surrounding the hard sphere, with a thickness of δ and a volume fraction

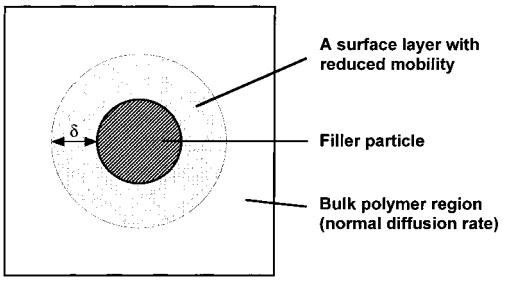

Figure 10. Drawing of a model for soft/hard blend films: we assume that there is a high-T_g polymer layer, of thickness δ, adjacent to the hard-particle surface. This layer has a reduced average diffusion rate (k'), surrounded by a region having the same mobility as the pure polymer ($k°$).

of PBMA f', that has reduced mobility, characterized by an average diffusion rate k'. The contribution to the fraction of mixing from this rigid part after time t is ($f'k't^{1/2}$). We assume that the rest of PBMA further from the hard phases has the same mobility as pure PBMA and therefore contributes $(1 - f')k°t^{1/2}$ to the mixing. Thus, in blend films

$$f_m = (1 - f')k°t^{1/2} + f'k't^{1/2} \quad (5)$$

Since the volume of the rigid layer is related to the hard-phase volume by $6\delta/d_{PMMA}$ and the volume ratio of PMMA to PBMA for our samples is 0.35/0.65, we obtain

$$f' = (0.35 \times 6\delta)/(0.65d_{PMMA}) = 3.2\delta/d_{PMMA} \quad (6)$$

Equation 5 can then be rewritten as

$$(f_m/t^{1/2}) = k° - 3.2(k° - k')\delta/d_{PMMA} \quad (7)$$

Equation 7 predicts that the global diffusion rate ($f_m/t^{1/2}$) decreases as d_{PMMA}^{-1}, i.e., is proportional to the surface area-to-volume ratio of the hard spheres. In Figure 11 we plot the values of $f_m/t^{1/2}$, obtained from the slopes of various sets of data in Figure 9, vs $1/d_{PMMA}$. A straight line is obtained. This indicates that a simple surface-rigidification model can explain the retardation effects of hard particles on PBMA diffusion observed in our experiments.

The linear fit in the $f_m/t^{1/2}$ vs $1/d_{PMMA}$ plot in Figure 11 gives an intercept of 0.089 $min^{-1/2}$ and a slope of -2.3 nm^{-1}. The intercept corresponds to $k°$, and its magnitude is not far from the $k°$ value determined for the pure PBMA sample (0.107 $min^{-1/2}$ from the data in Figure 9). From eq 7 and the slope in Figure 11, we obtain

$$(k° - k')\delta = 0.72 \quad (8)$$

In eq 8, $k°$ is known (0.1 $min^{-1/2}$ from Figures 9 and 11), whereas both δ and k' are unknown. Despite the simplicity of the model, we need an independent measurement to be able to calculate the individual parameters. Nevertheless, some deeper insights are possible. For example, k' must be larger than zero; thus, $\delta > 7.2$ nm. From the work of Zheng et al.[25] and Tsagaropoulos and Eisenberg,[32] one expects the retardation effect to depend on the molecular weight of the matrix polymer, and the span of δ should be related to the molecular dimensions of the polymer. Eisenberg et al.[38] assumed a distance on the order of the persistence length of the bulk polymer, to illustrate the reduction of molecular

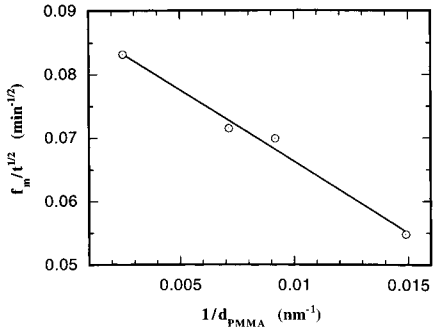

Figure 11. Plot of $f_m/t^{1/2}$ vs $1/d_{PMMA}$ in PBMA/PMMA blend films ($\Phi_{hard} = 0.35$). The data were derived from Figure 9.

mobility in the region surrounding high-T_g ion clusters in ionomer films. In the case of diffusion, the distance could be larger, since the entire molecule can experience retardation during movement, even if the restricted layer has a size only corresponding to a portion of the molecule. Let us assume that δ could be comparable to the diameter of the polymer coil in bulk, or twice the radius of gyration (R_G). For our PBMA sample of M_w = 35 000, the mean R_G is estimated to be 5.6 nm, calculated from the formula R_G (Å) = $0.30M_w^{1/2}$ for methacrylate polymers.[39] If we assume δ = 11.2 nm, we obtain a k' value of 0.036 min^{-1} in the restricted molecular layer, corresponding to about $^1/_3$ of the $k°$ value for the pure polymer.

In our simple model (Figure 11), we averaged into a single layer the effects of all the regions near the surface of varying degrees of mobility, including the possible existence of either an immobilized layer[32] or a less dense zone.[36] With respect to the immobilized layer, the diffusion results in our systems show a behavior very different from that of the Tsagaropoulos and Eisenberg DMA experiments on silica-filled polymers. They found that the area of the higher-T_g peak in the tan δ curve decreases by almost an order of magnitude at 20 wt % silica content, implying a large fraction of immobilized polymer. Our diffusion experiments show that PBMA can reach almost complete mixing in blend films ($f_m \approx$ 1) in our experiments. It would be interesting to conclude that a polymer which appears to be immobilized in a DMA experiment still has sufficient mobility to undergo translational diffusion, albeit on a longer time scale. Such a conclusion is premature, since the interaction between the silica filler and the matrix polymers examined by Tsagaropoulos and Eisenberg may be much stronger than the interactions between PMMA filler particles and PBMA. It will be interesting in future experiments to examine the effect of inorganic fillers on the diffusion rate of polymers in latex films.

Conclusions

We employed the fluorescence energy-transfer technique to measure the diffusion rate of poly(butyl methacrylate) (PBMA) at 60 °C in films blended with either PMMA or Ropaque hard particles. The hard particles significantly retard the diffusion rate of PBMA. The apparent diffusion coefficient (D_{app}) decreased from 0.3 to 0.2 nm^2/s at 35 vol % ROP and to 0.1 nm^2/s at 75 vol % ROP. Similar-sized PMMA (400 nm) particles gave similar retardation effects, with the D_{app} values slightly smaller than those in the ROP-filled films of the same hard-particle volume fraction. The diffusion rate decreases with an increase in the surface area of the hard

particles, i.e., with a decrease in the hard particle size at constant filler volume. We propose that there exists a rigid PBMA layer near the hard-particle surface which has lower mobility and a slower diffusion rate. This surface-rigidification model fits well to our experimental data.

Acknowledgment. We thank ICI, ICI Canada, and NSERC Canada for their financial support and Dr. S. Downing at ICI Paints (Slough, U.K.) for suggesting this project to us.

References and Notes

(1) Whitlow, J.; Wool, R. P. *Macromolecules* **1991**, *24*, 5926.
(2) (a) Wool, R. P.; O'Conner, K. M. *J. Appl. Phys.* **1981**, *52*, 5194, 5993. (b) Kim, Y. H.; Wool, R. P. *Macromolecules* **1983**, *16*, 1115.
(3) (a) Linné, M.; Klein, A.; Miller, G.; Sperling, L. H.; Wignal, G. *J. Macromol. Sci. Phys.* **1988**, *B27* (2 & 3), 217. (b) Yoo, J.; Sperling, L. H.; Glinka, C.; Klein, A. *Macromolecules* **1990**, *23*, 3962. (c) Yoo, J.; Sperling, L. H.; Glinka, C.; Klein, A. *Macromolecules* **1991**, *24*, 2868. (d) Mohammadi, N.; Yoo, J.; Klein, A.; Sperling, L. H. *J. Polym. Sci., Part B: Polym. Phys.* **1992**, *30*, 1311. (e) Kim, K.; Sperling, L.; Klein, A.; Wignall, G. *Macromolecules* **1993**, *26*, 4624.
(4) (a) Wang, Y.; Winnik, M. A. *Macromolecules* **1993**, *26*, 3147. (b) Li, L.; Wang, Y.; Feng, J.; Winnik, M. A.; Yan, H.; North, T., to be submitted for publication.
(5) (a) Wang, Y.; Zhao, C.; Winnik, M. A. *J. Chem. Phys.* **1991**, *95*, 2143. (b) Wang, Y.; Winnik, M. A.; Haley, F. *J. Coat. Technol.* **1992**, *64* (811), 51. (c) Kim, H.; Wang, Y.; Winnik, M. A. *Polymer* **1994**, *35*, 1779. (d) Kim, H.; Winnik, M. A. *Macromolecules* **1994**, *27*, 1007.
(6) (a) Hahn, K.; Ley, G.; Schuller, H.; Oberthur, R. *Colloid Polym. Sci.* **1986**, *264*, 1092. (b) Hahn, K.; Ley, G.; Oberthur, R. *Colloid Polym. Sci.* **1988**, *266*, 631. (c) Zosel, A.; Ley, G. *Macromolecules* **1993**, *26*, 2222.
(7) (a) Voyutskii, S. *J. Polym. Sci., Part A* **1958**, *32*, 528. (b) Voyutskii, S. *Autohesion and Adhesion of High Polymers*; Wiley: New York, 1963.
(8) Vanderhoff, J.; Bradford, E. B.; Carrington, W. K. *J. Polym. Sci., Polym. Symp.* **1973**, No. 41, 155.
(9) Winnik, M. A. The Formation and Properties of Latex Films. In *Emulsion Polymerization and Emulsion Polymers*; El-Aasser, M., Lovell, P., Eds.; Wiley: New York, 1997.
(10) Kowalski, A.; Vogel, M.; Blankenship, J. (Rohm Haas). European Patent 22 633, 1980.
(11) Rohm and Haas Reports on Ropaque Modified Polymer. *Resin Rev.* **1986**, *36* (3); **1987**, *37* (2); **1989**, *39* (2).
(12) (a) Feng, J.; Winnik, M. A. *Macromolecules* **1995**, *28*, 7671. (b) Winnik, M. A.; Feng, J. *J. Coat. Technol.* **1996**, *68* (852), 39.
(13) Feng, J.; Winnik, M. A. *Macromolecules* **1997**, *30*, 4324.
(14) Feng, J. Molecular and Environmental Aspects of Latex Film Formation. Ph.D. Thesis, University of Toronto, Toronto, Canada, 1997.
(15) O'Connor, D. V.; Phillips, D. *Time-correlated Single Photon Counting*; Academic: New York, 1984.
(16) Feng, J.; Yekta, A.; Winnik, M. A. *Chem. Phys. Lett.* **1996**, *260*, 296.
(17) (a) Joanicot, M.; Wong, K.; Maquet, J.; Chevalier, Y.; Pichot, C.; Graillat, C.; Lindner, P.; Rios, L.; Cabane, B. *Prog. Colloid Polym. Sci.* **1990**, *81*, 175. (b) Chevalier, Y.; Pichot, C.; Graillat, C.; Joanicot, M.; Wong, K.; Lindner, P.; Cabane, B. *Colloid Polym. Sci.* **1992**, *270*, 806.
(18) (a) Roulstone, B.; Wilkinson, M.; Hearn, J.; Wilson, A. *J. Polym. Int.* **1991**, *24*, 87. (b) Roulstone, B.; Wilkinson, M.; Hearn, J. *J. Polym. Int.* **1992**, *27*, 43.
(19) Wang, Y.; Kats, A.; Juhué, D.; Winnik, M. A.; Shivers, R.; Dinsdale, C. *Langmuir* **1992**, *8*, 1435.
(20) Dhinojwala, A.; Torkelson, J. *Macromolecules* **1994**, *27*, 4817.
(21) (a) Liu, Y.; Feng, J.; Winnik, M. A. *J. Chem. Phys.* **1994**, *101*, 9096. (b) Liu, Y.; Winnik, M. A. *Makromol. Chem. Symp.* **1995**, *92*, 321.
(22) (a) Yekta, A.; Duhamel, J.; Winnik, M. A. *Chem. Phys. Lett.* **1995**, *235*, 119. (b) Farinha, J.; Martinho, J. M.; Yekta, A.; Winnik, M. A. *Macromolecules* **1994**, *27*, 4817.
(23) Crank, J. *The Mathematics of Diffusion*; Clarendon: Oxford, U.K., 1974.
(24) (a) We emphasize that polymer diffusion in latex films can occur over distances much larger than the scale of the original particle diameters. The energy-transfer technique has its signal saturated ($f_m \rightarrow 1$) when the mean polymer diffusion distance is comparable to a particle radius. (b) Small changes in oven temperature can lead to differences in D_{app} values in experiments carried out several weeks apart. Temperature drift is normally not important, but when the oven temperature is reset, it is difficult to obtain precisely the same temperature. Bulk diffusion rates of PBMA are very sensitive to temperature. A higher molecular weight sample ($T_g = 30$ °C) has an apparent activation energy for diffusion of 160 kJ/mol in this temperature range.[5a]
(25) Zheng, X.; Sauer, B.; Alsten, J.; Schwarz, S.; Rafailovich, M.; Sokolov, J.; Rubinstein, M. *Phys. Rev. Lett.* **1995**, *74*, 407.
(26) (a) O'Brien, J.; Cashell, E.; Wardell, G.; McBrierty, V. J. *Macromolecules* **1976**, *9*, 653. (b) Douglass, D.; McBrierty, V. J. *Polym. Eng. Sci.* **1979**, *19*, 1054.
(27) Ito, M.; Nakamura, T.; Tanaka, K. *J. Appl. Polym. Sci.* **1985**, *30*, 3493.
(28) Dutta, N.; Choudhury, N.; Haidar, B.; Vidal, A.; Donnet, J.; Delmotte, L.; Chezeau, J. *Polymer* **1994**, *35*, 4293.
(29) Pliskin, I.; Tokita, N. *J. Appl. Polym. Sci.* **1972**, *16*, 473.
(30) Yim, A.; Chahal, R.; St. Pierre, L. *J. Colloid Interface Sci.* **1973**, *43*, 583.
(31) Landry, C.; Coltrain, B.; Landry, M.; Fitzgerald, J.; Long, V. *Macromolecules* **1993**, *26*, 3702.
(32) (a) Tsagaropoulos, G.; Eisenberg, A. *Macromolecules* **1995**, *28*, 396. (b) Tsagaropoulos, G.; Eisenberg, A. *Macromolecules* **1995**, *28*, 6067.
(33) Alter, H. *J. Appl. Polym. Sci.* **1965**, *9*, 1525.
(34) Lewis, T.; Nielsen, L. *J. Appl. Polym. Sci.* **1970**, *14*, 1449.
(35) (a) Sumita, M.; Ookuma, T.; Miyasaka, K.; Ishikawa, K. *J. Appl. Polym. Sci.* **1982**, *27*, 3059. (b) Sumita, M.; Tsukumo, Y.; Miyasaka, K.; Ishikawa, K. *J. Mater. Sci.* **1983**, *18*, 1758. (c) Sumita, M.; Ookuma, T.; Miyasaka, K.; Ishikawa, K. *J. Appl. Polym. Sci.* **1984**, *29*, 1523.
(36) (a) Vollenberg, P.; Heikens, D. *Polymer* **1989**, *30*, 1656. (b) Vollenberg, P.; de Haan, J.; van de Ven, L.; Heikens, D. *Polymer* **1989**, *30*, 1663.
(37) van Krevelen, D. *Properties of Polymers*; Elsevier: Amsterdam, The Netherlands, 1972.
(38) Eisenberg, A.; Hird, B.; Moore, R. *Macromolecules* **1990**, *23*, 4098.
(39) Kirste, R.; Kruse, W.; Ibel, K. *Polymer* **1975**, *16*, 120.
(40) Keddie, J. L.; Jones, R. A. L.; Cory, R. A. *Faraday Discuss.* **1994**, *98*, 219; *Europhys. Lett.* **1994**, *27*, 59.
(41) Wallace, W. E.; van Zanten, J. H.; Wu, W. *Phys. Rev. E.* **1995**, *52*, R3329; van Zanten, J. H.; Wallace, W. E.; Wu, W. *Phys. Rev. E.* **1996**, *53*, R2053.
(42) (a) Forrest, J. A.; Dalnoki-Veress, K.; Stevens, J. R.; Dutcher, J. R. *Phys. Rev. Lett.* **1996**, *77*, 2002. (b) Forrest, J. A.; Dalnoki-Veress, K.; Dutcher, J. R.; Rowat, A. C.; Stevens, J. R. *Mater. Res. Soc. Symp. Proc.* **1996**, *407*, 131. (c) Forrest, J. A.; Rowat, A. C.; Dalnoki-Veress, K.; Stevens, J. R.; Dutcher, J. R. *J. Polym. Sci., Part B: Polym. Phys.* **1996**, *34*, 3009.
(43) Mansfield, K. F.; Theodorou, D. N. *Macromolecules* **1991**, *24*, 6283.
(44) Baschnagel, J.; Binder, K. *Macromolecules* **1995**, *28*, 6808.
(45) Keddie, J. L.; Cory, R. A.; Jones, R. A. L. In *Modern Aspects of Colloidal Dispersions*; Ottewill, R. H., Rennie, A. R., Eds.; Kluwer Academic Publishers: London, 1998; pp 149−158.
(46) Frank, B.; Gast, A. P.; Russell, T. P.; Brown, H. R.; Hawker, C. *Macromolecules* **1996**, *29*, 6531.
(47) Sullivan, D. A. *J. Paint Technol.* **1975**, *47* (610), 60.
(48) Eckersley, S.; Helmer, B. *J. Coat. Technol.* **1997**, *69* (864), 97.

MA980117W